INSTITUTIONEN FÖR
VÄRME- OCH KRAFTTEKNIK

TEKNISKA HÖGSKOLAN I LUND

The Effect of Valve Strategy on In-Cylinder Flow and Combustion

Fredrik Söderberg

ISBN 0282-1990
ISRN LUTMDN/TMVK--5280--SE

DEPARTMENT OF HEAT AND POWER ENGINEERING
LUND INSTITUTE OF TECHNOLOGY
P.O. BOX 118, S-221 00 LUND
SWEDEN

Dokumentutgivare
LU/LTH, Inst. för Värme- och Kraftteknik

Dokumentnamn
Examensarbete

Dokumentbeteckning
ISRN LUTMDN/TMVK-5280—SE

Handläggare
Bengt Johansson

Utgivningsdatum
Jan 1997

Ärendebeteckning

LUTMDN-TMVK--5280

Författare:
Fredrik Söderberg

Dokumenttitel och undertitel:

The Effect of Valve Strategy on In-Cylinder Flow and Combustion

Referat (abstract):

This paper examines the effects of different valve strategies and their effect on in-cylinder flow and combustion. A conventional four valve per cylinder Otto engine was modified to enable optical access. The flow measurements were made with a two-component laser Doppler velocimetry system. The combustion was monitored by running pressure data from a pressure transducer through a one-zone heat release model.

The results show that when the valves operate normally a barrel flow is present and when one valve is closed a swirling flow occurs. No increase in turbulence was found with later phasing, except in the case of very late inlet valve opening and port deactivation. This resulted in a jet with high turbulence, making the combustion fast and stable, even with a very lean mixture ($\lambda = 1.8$).

Referat skrivet av:
Författaren

Förslag till ytterligare nyckelord

Klassifikationssystem och -klass(er)

Indextermer (ange källa)

Omfång:
21 sidor + 11 sidor appendix

Övriga bibliografiska uppgifter

Språk:
Engelska

Sekretessuppgifter

ISSN
0282 - 1990

ISBN

Dokumentet kan erhållas från
Inst. för Värme- och Kraftteknik
Box 118
Lund

Mottagarens uppgifter

Pris

RB

Acknowledgments

The experiments in this paper were carried out in the summer of 1995. It was very hot outside and the air conditioning was a blessing. The results in the paper were first published at the SAE congress in Detroit in February 1996, by my supervisor Bengt Johansson. I would like to thank him for his assistance and guidance throughout this work.

I would also like to thank Bertil Andersson, who handles the engine and the experimental setup. If there was ever a problem to solve, Bertil solved it.

No experimental data could have been recorded if it had not been for Krister Olsson. He handled the HP-logger and backup service eminently.

Furthermore, I would like to thank my colleague and friend Martin Ekenberg for making life difficult for me by asking me tricky questions about my laboratory setup.

Abstract

This paper examines the effects of different valve strategies and their effect on in-cylinder flow and combustion. A conventional four valve per cylinder otto engine was modified to enable optical access. The flow measurements were made with a two-component laser Doppler velocimetry system. The combustion was monitored by running pressure data from a pressure transducer through a one-zone heat release model.

The results show that when the valves operate normally a barrel flow is present and when one valve is closed a swirling flow occurs. No increase in turbulence was found with later phasing, except in the case of very late inlet valve opening and port deactivation. This resulted in a jet with high turbulence, making the combustion fast and stable, even with a very lean mixture ($\lambda = 1.8$).

1 Introduction

Normal valve timing is a compromise between stable idle and high performance. Optimum idle timing means little valve overlap (giving little internal exhaust gas recirculation, EGR) and early inlet valve closing (close to bottom dead center, BDC). Optimum timing for high performance means large overlap and late inlet valve closing, which makes full use of inertia effects of the inlet charge. The valve timing chosen depends on the characteristic of the vehicle. One extreme example is the formula one car which is unable to run at speeds below approximately 5000 rpm. Variable valve timing is a way of achieving both stable idle and optimum performance.

There are several different ways of obtaining variable valve timing, e.g. port deactivation, which is used by Honda VTEC-E [1] and inlet cam phasing, which is used by Mercedes [2]. Hydraulic lifters, controlled by solenoids, is a new concept developed by Ford [3]. This camless engine makes new engine strategies possible, e.g. deactivating one or more cylinders at part load and thereby reducing pumping mean effective pressure, PMEP. Another way of reducing PMEP at part load is to use the Miller cycle, which means that very early/late inlet valve closing is used, making the expansion ratio greater than the compression ratio. This is used by Nissan in their top-of-the-line car Maxima [4].

The purpose of studying variable valve timing is to increase the efficiency of the engine. This makes it possible to produce smaller engines without loosing performance, which renders better fuel economy. Another option is to increase the performance of the engine without making it larger. This paper studies the effects of variable valve timing on a single cylinder, four valves per cylinder otto engine, running on natural gas. No information is given as to how variable valve timing should be achieved.

1.1 Valve timing

The choice of valve timing is depending on the characteristic wanted from the engine. Several parameters can be changed and they all effect the behavior of the engine. This section describes the influence of valve timing.

1.1.1 Exhaust valve opening

The exhaust valve is opened at the end of the expansion stroke in order to evacuate the exhaust gases. If the exhaust valve is opened to late, e.g. at BDC, the piston must push the high pressure gases out and great losses are made. If instead the exhaust valve is opened before BDC the pressure in the cylinder blows out the exhaust gases. This is called blow down. Thereafter the piston pushes the remaining low pressure exhausts out through the exhaust valve and less work is lost. Due to the early opening of the exhaust valve, the expansion stroke is reduced, but this is during the late phase of the stroke where the piston is inefficient in transferring work to the crank shaft; hence a gain in efficiency is made. The exhaust opening time of a normal personal car is 40 crank angle degrees before BDC.

1.1.2 Inlet valve opening

When the piston has pushed out all of the exhaust gases, the cylinder must be filled with fresh charge. Since the exhaust gases are flowing out of the

cylinder the combustion chamber is at slight vacuum due to the inertia of the exhaust gases. This suction can be used to increase the volumetric efficiency (i.e. the amount of fresh charge in the cylinder compared to the theoretical full charge at atmospheric pressure). This is accomplished by opening the inlet valve before top dead center. Too early inlet valve opening enables the exhaust gases to enter the inlet manifold. This is even more likely during part load when the inlet manifold is at low pressure. The dilution of the fresh charge with exhaust gases deteriorates the combustion in the next cycle, making the exhaust gases rich with CO and unburned hydrocarbons, HC. A compromise must be made for the engine application in question.

1.1.3 Exhaust valve closing

Since it is the inertia of the exhaust gases that creates the positive suction of the fresh charge, the exhaust valve must remain open some time after opening the inlet valve. This is called valve overlap. The optimum duration of the overlap is depending on engine speed and load. At part load, the low pressure of the inlet manifold can draw exhaust gases from the exhaust manifold into the cylinder and further back into the inlet manifold. The inertia of the exhaust gases prevents this but only at higher engine speeds. Again a compromise must be made to make the engine operating at different speeds and loads.

1.1.4 Inlet valve closing

When the piston is moving down during the charging stroke, the fresh charge is drawn from the inlet manifold into the cylinder. At low engine speeds the optimum inlet valve closing time is at bottom dead center. However, at higher engine speeds the inertia of the inlet charge makes it possible to press more charge into the cylinder and thus increase the volumetric efficiency. During low engine speeds, the volumetric efficiency will decrease due to the later inlet valve closing. The normal closing time chosen in personal cars is 50 crank angle degrees after BDC.

1.2 Other influencing factors

Asymmetric valve timing promotes a swirling flow in the cylinder. This increases the turbulence and makes the combustion faster and more stable. High valve lift, however, results in a barrel swirl called tumble. This kind of in-cylinder flow is often seen in a four valve per cylinder otto engine. The turbulence is increased at TDC due to the breakdown of the tumble.

Honda VTEC-E is a normal four valves per cylinder engine with controllable valve deactivation. One of the valves can be deactivated by closing a throttle in one of the inlet ports. This is done at part load and at low speeds when the air flow is moderate. The valve deactivation increases the turbulence without influencing the performance at full load and speed.

As can be seen, the valve timing of an engine is depending on engine speed and load, and this has been known for a long time. Today, engine manufacturers are beginning to make use of the variable valve timing technology. Some ideas are small modifications that make some improvements in engine efficiency, e.g. Mercedes who use inlet cam phasing to improve valve timing, and other ideas are fundamentally new. Fords new

camless engine, which recycles the hydraulic oil used to control the valves, is more efficient than the ordinary cam shaft.

2 Experimental apparatus

This section describes the engine and the auxiliary equipment needed for the experiments. It also describes how some of the measurement techniques work.

2.1 Engine

The engine is a single cylinder version of the Volvo B5254 five cylinder engine. Its geometric properties are given in Table 1. This single cylinder version still had all five pistons and cylinders remaining and moving without firing, which makes it a one cylinder engine with the frictional losses of a normal five cylinder engine.

Table 1: The geometric properties of the engine

Displaced volume	487 cm^3
Bore	83 mm
Stroke	90 mm
Offset	0.8 mm
Compression ratio	10:1

The engine has a pent roof combustion chamber, which enables tumble flow and makes it compact. Two different cam shafts were used: the standard inlet cam shaft and a modified inlet cam shaft with only one cam lobe. The modified cam represents valve deactivation. Variable valve timing was achieved by setting the cam belt on wrong on the cam wheel. The number of teeth wrong decided the phasing. Table 2 specifies the different valve timings used in this paper.

Table 2: The valve timings used in this paper. The abbreviation TDC stands for top dead center and the abbreviation BDC stands for bottom dead center. The prefix A and B stands for after and before, respectively.

Camshaft	Valve open (CAD)	Valve close (CAD)	Overlap (CAD)
Exhaust	44.0 BBDC	16.0 ATDC	
Inlet standard	8.0 BTDC	52.0 ATDC	24.0
Inlet late one	9.1 ATDC	69.1 ABDC	6.9
Inlet late two	26.3 ATDC	86.3 ABDC	-18.3
Inlet late three	43.4 ATDC	103.4 ABDC	-35.4

In order to make velocity measurements optical access was required. This was obtained by drilling holes in the side of the pent roof combustion chamber and inserting small quartz windows (see Fig. 1). This reduced the compression ratio by 0.4 units but was not considered to influence in-cylinder flow. During the pressure measurements, one of the windows was replaced by a pressure transducer.

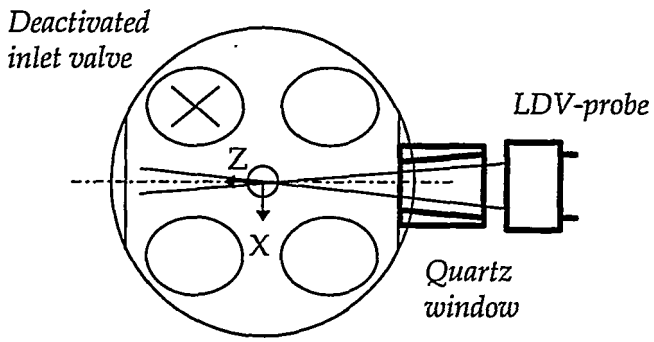

Figure 1: This is the cylinder head seen from below. It displays the arrangement for optical access and the coordinate system for the velocity measurements. The Y direction is defined with positive values upwards.

2.2 LDV system

For the velocity measurements a two component Laser Doppler Velocimetry (LDV) system from DANTEC was used. This made it possible to measure the velocity in two orthogonal directions, named X and Y, and by traversing through the combustion chamber (in the Z-direction) a cross-section of the in-cylinder flow could be obtained.

2.3 LDV-technique

Laser Doppler Velocimetry is a non-intrusive velocity measurement technique. The working principle of LDV is to have laser beams crossing at a certain angle, which leads to an interference pattern. When a particle moves through the interference pattern it reflects the laser light each time it passes a fringe, and this signal is analyzed. Depending on the angle between the two laser beams and the wavelength of the laser light, there is a certain distance between the fringes in the interference pattern. By using the simple equation

$$s = v \cdot t \tag{1}$$

it is possible to calculate the velocity of the particle. By having two laser beam crossings, two velocity components can be measured.

In order to detect stationary particles, a phase-shift of one of the two laser beams is necessary. This makes the fringes moving at a certain velocity depending on the magnitude of the phase-shift. The LDV technique requires particles to scatter the incoming laser light. They are described more thoroughly later (operating conditions).

2.4 Pressure measurements

The pressure was monitored using a piezo-electric pressure transducer connected to a Kistler charge amplifier. This signal was sent to a 486 PC, via a HP-logger. By running the pressure data through a one-zone heat release model, the combustion rate was obtained. This makes it possible to calculate the rate of heat release, total heat release, ignition delay, combustion duration, indicated mean effective pressure (IMEP) and pumping mean effective pressure (PMEP). Ignition delay is the time for 0-10% heat release and combustion duration is the time for 10-90% heat release. Indicated mean effective pressure is a measure of the work delivered by the engine divided by engine size according to

$$\text{IMEP} = \frac{W_{c,i}}{V_d} \tag{2}$$

where $W_{c,i}$ is the indicated energy per cycle and V_d is the displacement of the cylinder in the engine.

2.5 Control system

The engine was controlled by a PC-based system which made it possible to vary ignition timing and skip-fire mode settings. Input signals to the control system was a sync pulse (one pulse per two revolutions), a TDC pulse and a crank angle degree signal (five pulses per crank angle degree).

3 Pressure system

The pressure system consists of a pressure transducer, a charge amplifier and a software for converting the signal from the pressure transducer into pressure.

3.1 Pressure transducer

Measuring the pressure in an engine demands advanced pressure transducers. It must be able to handle pressures ranging from 0.3 bar absolute (during the inlet stroke at part load) up to 150 bar (combustion in a supercharged diesel). The transducer must also be able to withstand high frequencies generated if the engine is operating with knock.

The most commonly used pressure transducer for automobile applications is the piezo-electric type. It produces an electrical signal proportional to the change in pressure. This makes it necessary to use specific software to convert the pressure signal into pressure data. The pressure transducer is also sensitive to mechanical vibrations and to rapid changes in temperature (called thermo shock). According to a test made by Klell and Wimmer [5], a pressure transducer from AVL, QC41B-X was the best choice in everything accept for the rather poor thermo shock protection. Since then, AVL has modified the transducer with better protection against thermo shock. This modified version, AVL QC42D-X, was used during the measurements.

3.2 Charge amplifier

The charge amplifier receives the voltage signal from the pressure transducer and amplifies it a specified amount. According to a test made by Bengt Johansson [6], the charge amplifiers had the levels of noise given in Table 3.

Table 3: Noise on the voltage output from different tested charge amplifiers. The pressure transducer was in all cases connected and mounted in the engine.

Charge amplifier	Noise RMS (mV)	Noise Peak-Peak (mV)
Kistler 5011	1.5	30
AVL 3056	1.2	20
Kistler 5001	0.3	3
Brüel & Kjaer	1.5	20

As can be seen in Table 3, the Kistler 5001 gave the lowest noise signal. The reason for this large difference is unknown. The newer version (Kistler 5011) was sent back to the supplier for a check, but it was found to be working satisfactory. The Kistler 5001 was chosen for all the measurements.

4 Operating conditions

The engine was run on natural gas. Its content can be seen in Table 4. During the experiments the engine speed was held constant at 1500 rpm. The pressure measurements were all made with an indicated mean effective pressure (IMEP,net) of four bar. This point was chosen as it represents the normal operating point of a passenger car. The choice of IMEP instead of BMEP was due to the special design of the single cylinder engine with frictional losses of a five cylinder engine.

Table 4: The contents of the natural gas used.

Component	Vol. %	Mass %
Methane	91.1	81.1
Ethane	4.7	7.9
Propane	1.7	4.2
n-Butane	1.4	4.7
Nitrogen	0.6	0.9
Carbon dioxide	0.5	1.2

The LDV system needed particles to reflect the light (called seeding), and these particles had to be added with the inlet air. A polystyrene-latex water dispersion was used with a mean particle size of 0.28 µm. This is considered small enough for the particles to follow the fluid flow in high turbulence.

As the seeding would burn up during normal fired operation, all LDV measurements had to be made during a motored cycle. In skip-fire mode the engine was fired for ten cycles and then motored one cycle. During the LDV measurements the engine was run at wide open throttle and stoichiometric air fuel ratio. This heated the windows enough to maintain a self cleaning effect.

5 Data processing

All engines have some cycle to cycle variations and to be able to get some valuable information out of the measurements, statistical analysis must be applied. This supplies a way of correlating different measurements against each other and determining the error made during the measurements. If the error is too great, the measurements have to be checked and perhaps new experiments have to be made.

The velocity registrations from the LDV measurements are treated by using a moving Hanning window. This technique calculates the weighted average over an interval of chosen width. This average is considered to be the mean velocity at the center of the interval. The next interval is then chosen at some time later and a new average is calculated. The average curve obtained through these calculations are called the mean velocity. The difference between the mean velocity and the velocity registrations are called high frequency turbulence. The length of the interval (i.e. the width of the Hanning window) determines the cut-off frequency between turbulence and mean

velocity. By changing the length of the interval, different cut-off frequencies can be used. The mean velocity and turbulence data is then ensemble-averaged for all the measured cycles for all engine configurations.

6 Flow results

The results will be presented for eight different configurations depending on valve timing and cam shaft type. The flow was measured along a line in the center of the combustion chamber. This results in a cross-section of the three-dimensional flow. The horizontal velocity component will show if swirl or squish is present and the vertical velocity component will show the barrel flow or tumble flow. Figure 2 shows the expected velocity profiles for the tumble and swirl flow, respectively. The average turbulence, according to

$$\text{average turbulence} = \sqrt{\frac{u'+v'}{2}} \tag{3}$$

is plotted as a function of crank angle degree for the different configurations. In (3), u' is the turbulence in the X-direction and v' is the turbulence in the Y-direction.

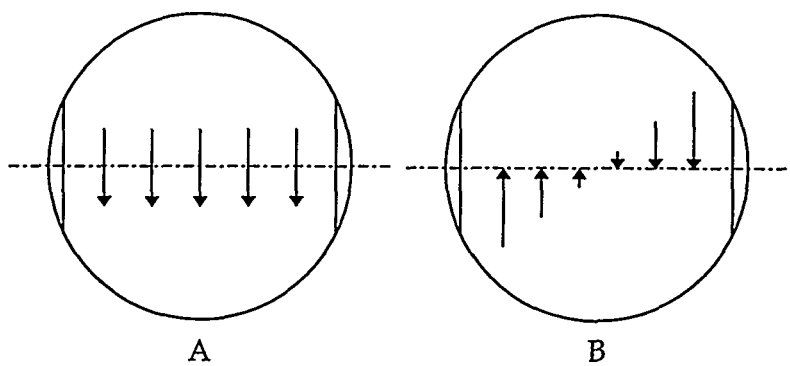

Figure 2: This is the cylinder seen from above. In A, the velocity registrations for the tumble flow is shown and in B, the velocity registrations for a swirling flow is shown.

6.1 Two inlet valves

This configuration corresponds to the normal double cam operation of this engine. It is designed to achieve tumble, which generates high turbulence during compression due to breakdown of the large flow.

MEAN VELOCITY- The mean velocity for the standard double cam for the normal valve timing can be seen in Fig. 3-4. The expected tumble flow can be seen clearly but is not very pronounced at the cylinder walls. This is probably due to the circular cross section of the cylinder. The vertical velocity component shows positive values before top dead center and negative afterwards. This is probably due to the compression and the following expansion. The magnitude of the vertical velocity is however small. With 17 crank angle degrees later inlet cam phasing, no significant difference can be seen (Fig. 6-7), but with still later phasing the horizontal velocity increased (Fig. 9-10). For the very late case, the vertical velocity showed the highest values at the cylinder walls (Fig. 12-13). This is in contradiction to the normal phase, but can be interpreted as a horizontal double vortex. However, information is lacking to make any certain conclusions.

The standard deviation of the mean velocity in the vicinity of the spark plug can be seen in Fig. 28. The figure shows that there is more variation in the two cases with very late inlet cam phasing which means less stability for these cases.

TURBULENCE- For the normal inlet cam phasing, the turbulence has a peak 20 crank angle degrees before top dead center (Fig. 5). This is expected due to the breakdown of the tumble flow. With later cam phasing, the peak before top dead center is less pronounced (Fig. 8, 11 and 14) and Fig. 27 shows that there is a decrease in turbulence in the vicinity of the spark plug for the very late cam phasing. This is surprising, as the very late phase was expected to create intense shear flow and hence increase the turbulence. The reason why this did not happen is believed to be the disturbance caused by the blow-back from the cylinder to the inlet manifold, caused by the very late inlet valve closing. This is also indicated by the reduced horizontal velocity and the lack of a turbulence peak before top dead center.

As can be seen in Fig. 29 there is no significant difference in standard deviation between the various cases in the vicinity of the spark plug.

6.2 Inlet valve deactivation

Valve deactivation has been reported to generate a swirling flow in the cylinder. This is also expected in this engine. In the measurements, a swirling flow will be plotted as a straight velocity gradient with positive horizontal velocities at negative Z coordinates and negative horizontal velocities at positive Z coordinates, according to Fig. 2. At the spark, a zero horizontal velocity is expected.

MEAN VELOCITY- Figures 15, 18, 21 and 24 show that a swirling flow is present at the beginning of the measurements. The swirl increases as the inlet cam is phased later, as expected. There is, however, an interesting effect close to top dead center – a velocity gradient with opposite sign to the predominant. This indicates an inner swirl rotating at the opposite direction.

The vertical flow shows the same trend as in the two inlet valve case, with positive values before top dead center and negative values after top dead center (see Fig. 16, 19, 22 and 25). The vertical velocity component also responds to the late inlet cam phase and the very late inlet cam phase shows very few similarities with the normal case.

The standard deviation of the mean velocity for inlet valve deactivation can be seen in Fig. 31 where the two cases with the largest retardation of the cam shaft have the highest values. This can also be seen in the irregular 3-D plots (Fig. 21, 22, 24 and 25). This is explained by the larger mean velocities for these cases which in turn means that the relative deviation is the same in all cases.

TURBULENCE- With valve deactivation, the turbulence is significantly increased (see Fig. 17, 20, 23 and 26). The turbulence still has a peak before top dead center, though. The three-dimensional landscapes have large irregularities, which indicates less homogeneity. Figure 30 shows the average level of turbulence in the vicinity of the spark plug as a function of crank angle degree with inlet valve deactivation. The turbulence increases for the two cases with the largest retardation of the phasing. In the very late cam phase case, the turbulence is twice as large as in the other cases with inlet cam deactivation.

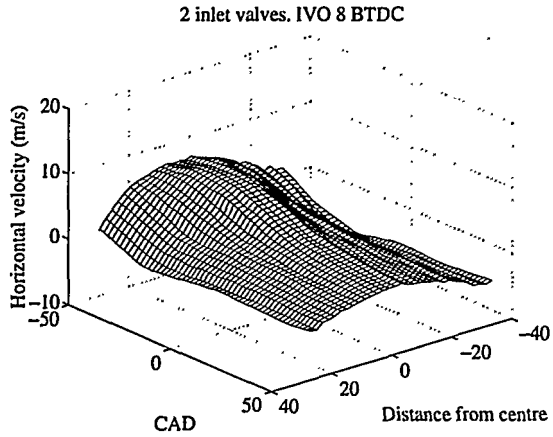

Figure 3: The horizontal velocity for two inlet valves and normal phase.

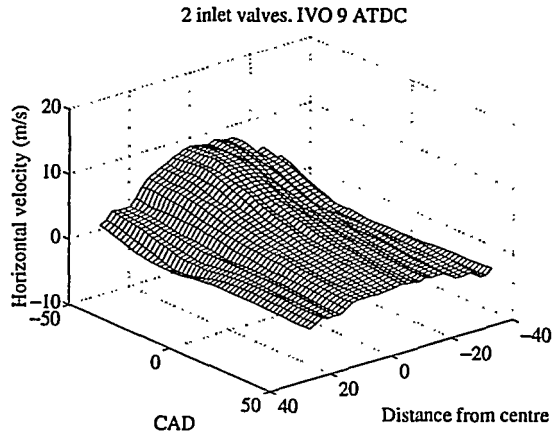

Figure 6: The horizontal velocity for two inlet valves and 17.1 CAD late phase.

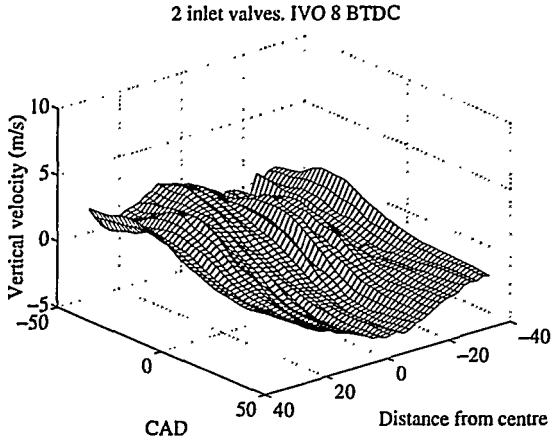

Figure 4: The vertical velocity for two inlet valves and normal phase.

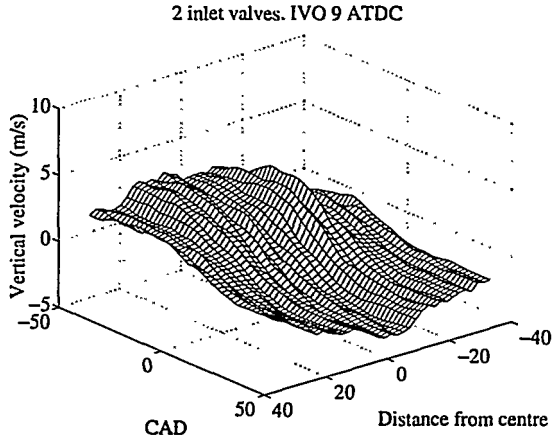

Figure 7: The vertical velocity for two inlet valves and 17.1 late phase.

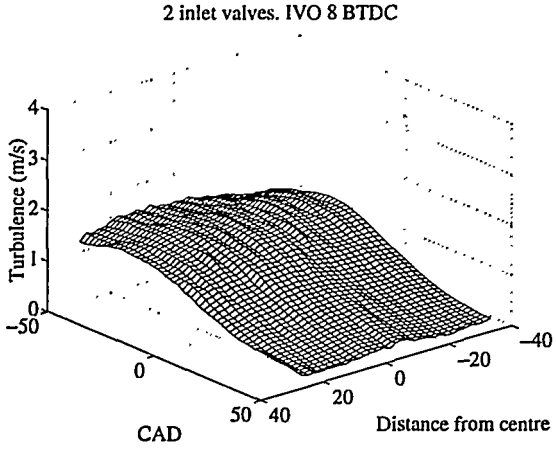

Figure 5: The turbulence for two inlet valves and normal phase.

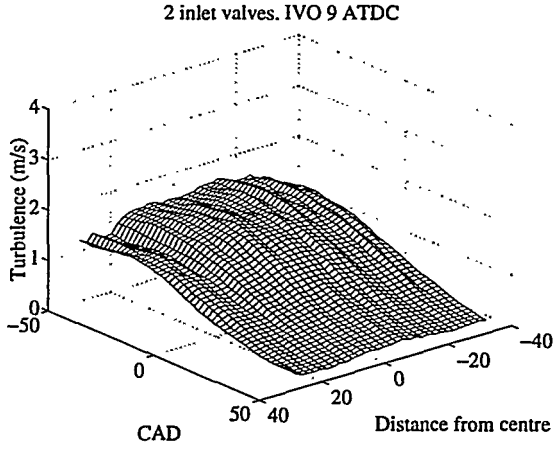

Figure 8: The turbulence for two inlet valves and 17.1 late phase.

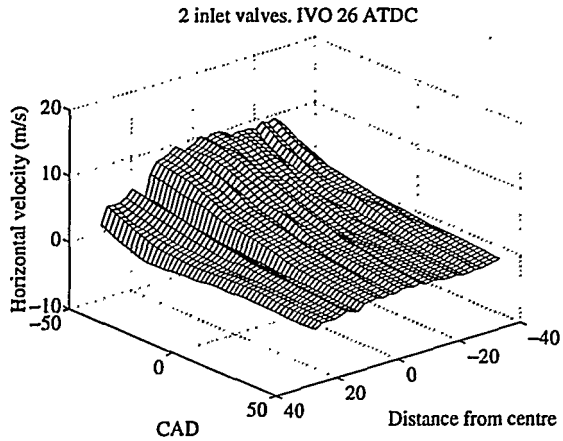

Figure 9: The horizontal velocity for two inlet valves and 34.3 CAD late phase.

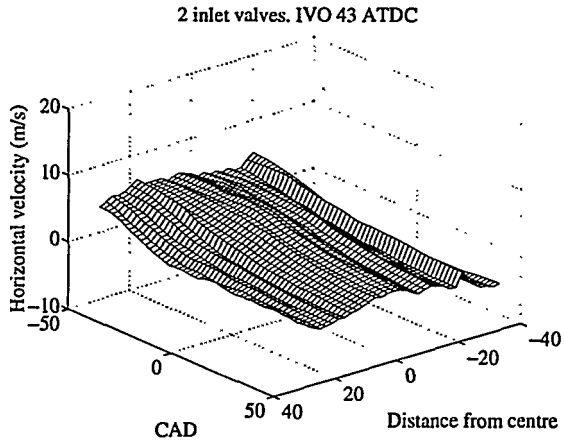

Figure 12: The horizontal velocity for two inlet valves and 51.4 CAD late phase.

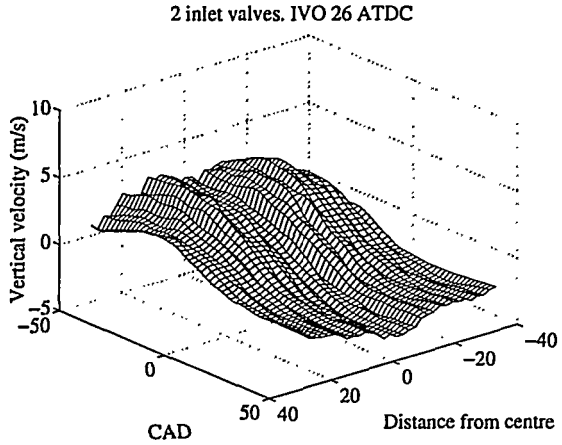

Figure 10: The vertical velocity for two inlet valves and 34.3 CAD late phase.

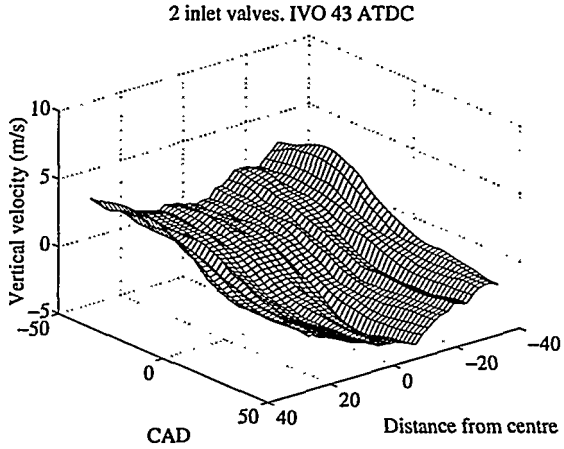

Figure 13: The vertical velocity for two inlet valves and 51.4 CAD late phase.

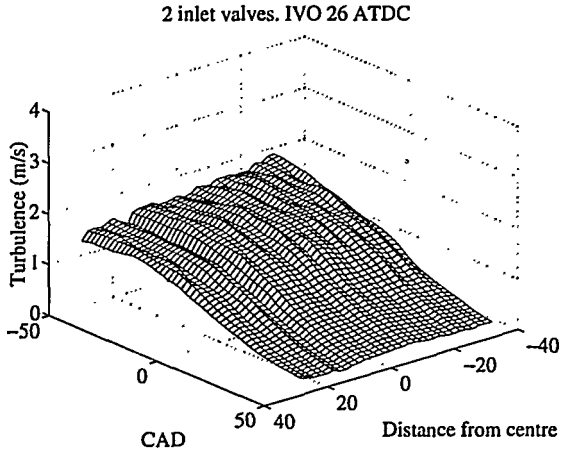

Figure 11: The turbulence for two inlet valves and 34.3 CAD late phase.

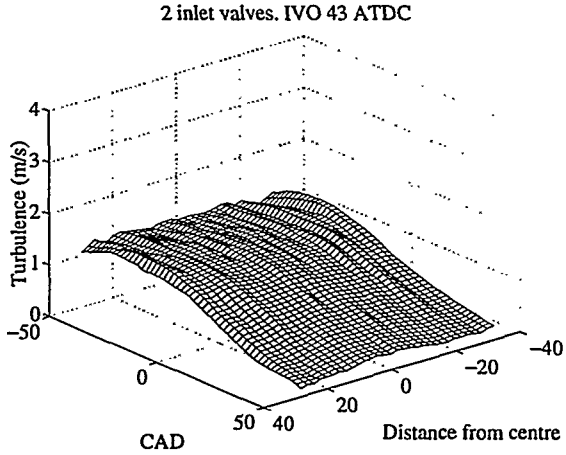

Figure 14: The turbulence for two inlet valves and 51.4 CAD late phase.

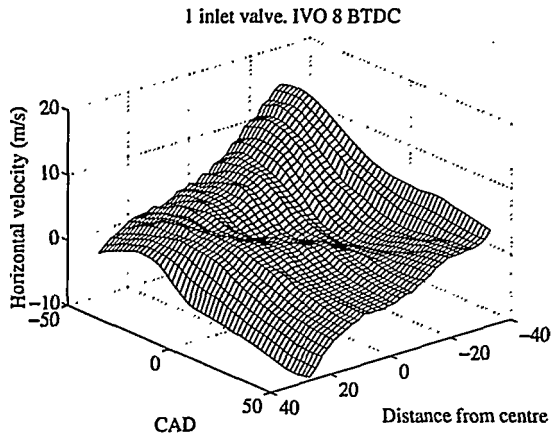

Figure 15: The horizontal velocity for one inlet valve and normal phase.

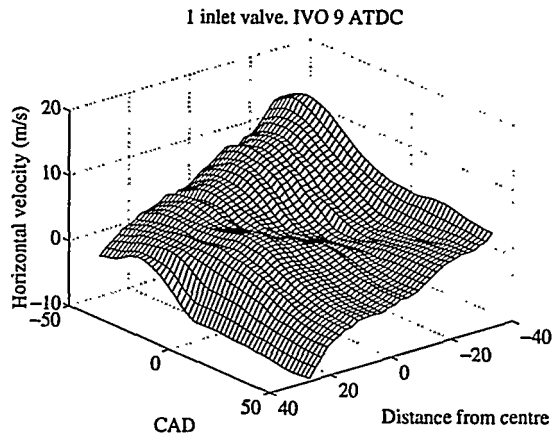

Figure18: The horizontal velocity for one inlet valve and 17.1 CAD late phase.

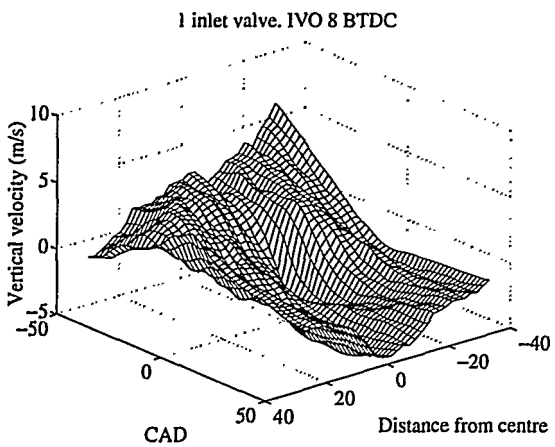

Figure 16: The vertical velocity for one inlet valve and normal phase.

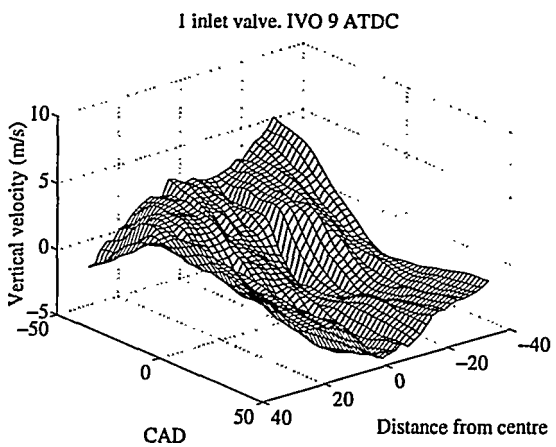

Figure 19: The vertical velocity for one inlet valve and 17.1 CAD late phase.

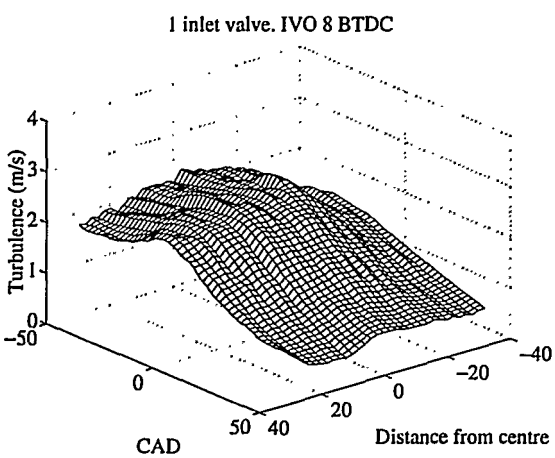

Figure 17: The turbulence for one inlet valve and normal phase.

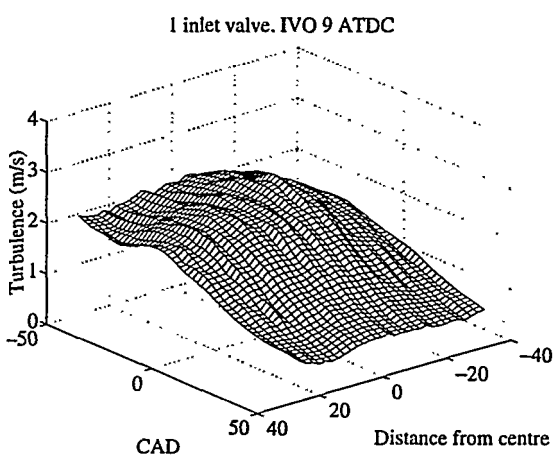

Figure 20: The turbulence for one inlet valve and 17.1 CAD late phase.

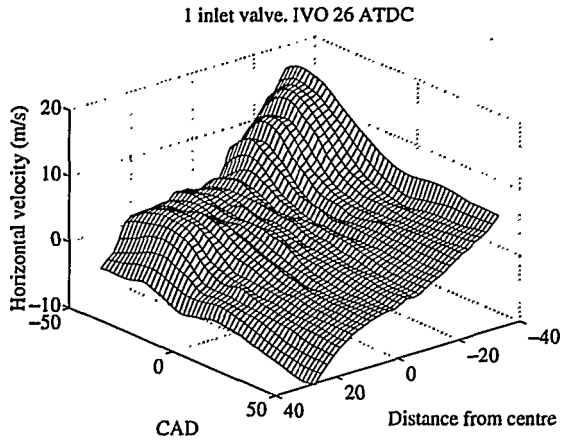

Figure 21: The horizontal velocity for one inlet valve and 34.3 CAD late phase.

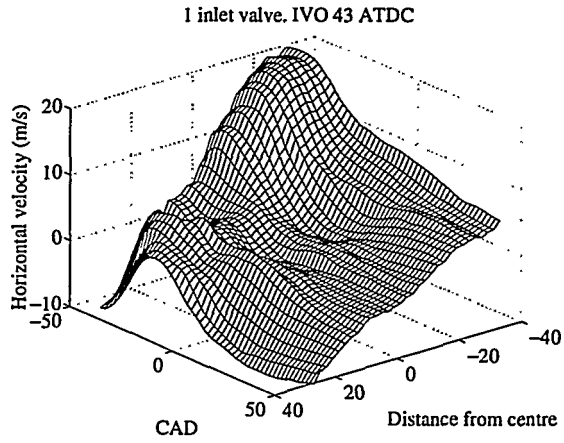

Figure 24: The horizontal velocity for one inlet valve and 51.4 CAD late phase.

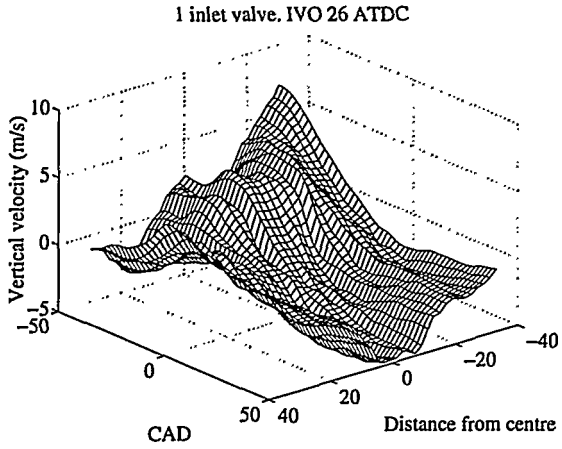

Figure 22: The vertical velocity for one inlet valve and 34.3 CAD late phase.

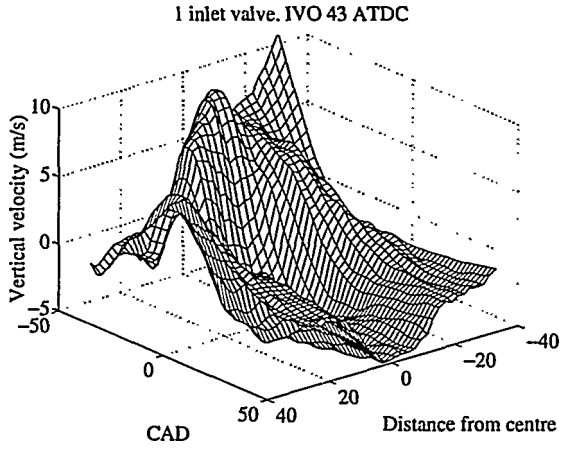

Figure 25: The vertical velocity for one inlet valve and 51.4 CAD late phase.

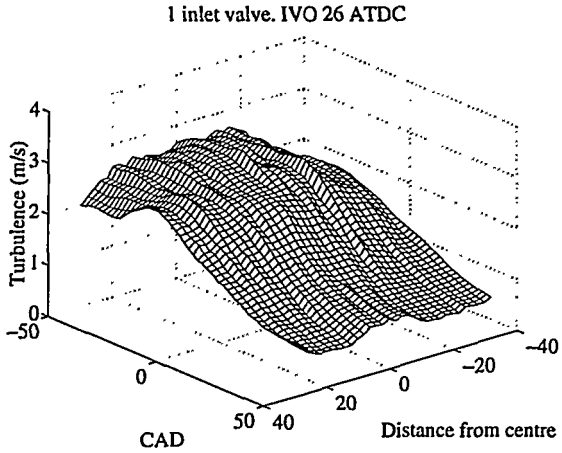

Figure 23: The turbulence for one inlet valve and 34.3 CAD late phase.

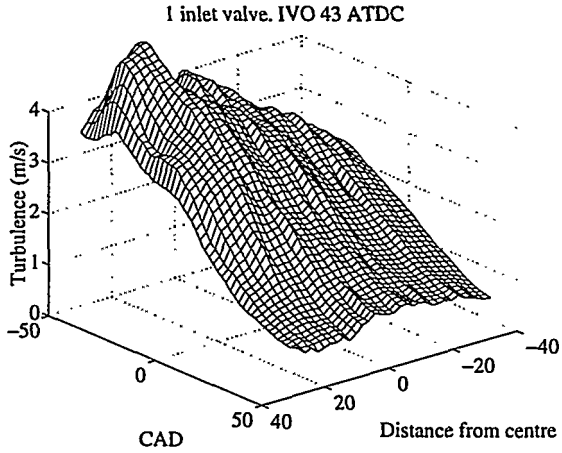

Figure 26: The turbulence for one inlet valve and 51.4 CAD late phase.

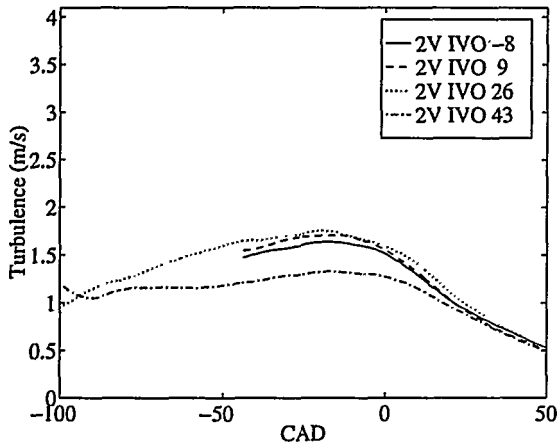

Figure 27: The turbulence in the vicinity of the spark plug for different inlet cam phases.

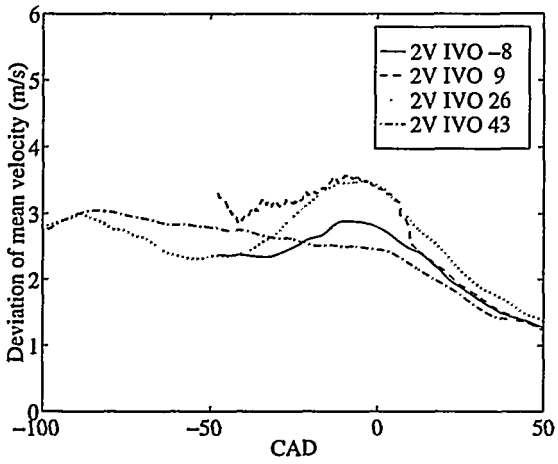

Figure 28: Standard deviation of mean velocity from cycle to cycle, in the vicinity of the spark plug.

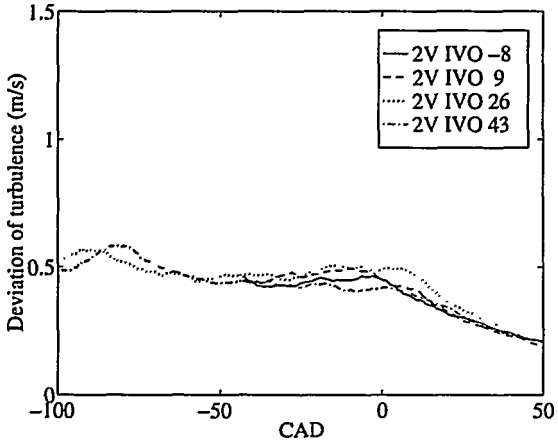

Figure 29: Standard deviation of turbulence from cycle to cycle, in the vicinity of the spark plug.

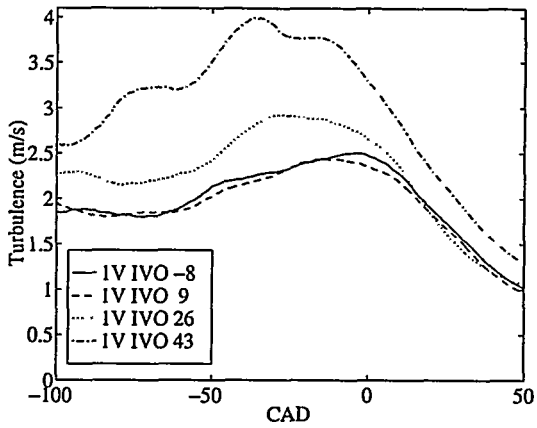

Figure 30: The turbulence in the vicinity of the spark plug for different inlet cam phases and inlet valve deactivation.

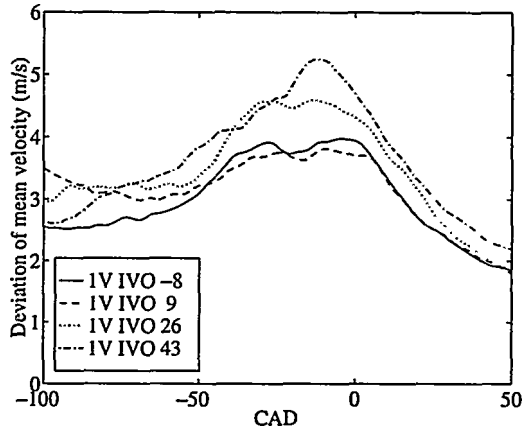

Figure 31: Standard deviation of mean velocity from cycle to cycle, in the vicinity of the spark plug and inlet valve deactivation.

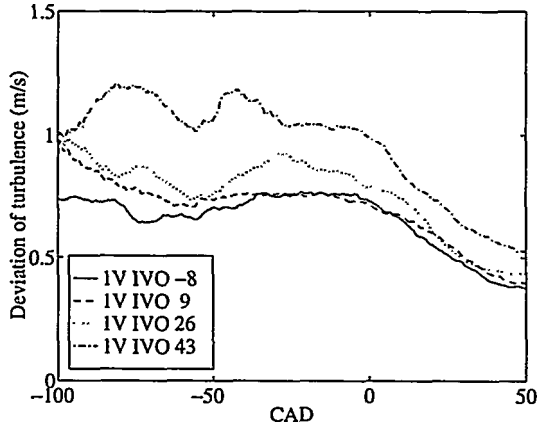

Figure 32: Standard deviation of turbulence from cycle to cycle, in the vicinity of the spark plug and inlet valve deactivation.

The standard deviation of the turbulence is also larger for the very late phasing case (Fig. 32), but again this is explained by the larger turbulence value.

7 Pressure results

By running the pressure data through a one-zone heat-release model, the pumping mean effective pressure, combustion duration and combustion stability can be determined. The pressure data as a function of crank angle degree can be seen in Fig. 33-36 showing the gas exchange phase for different valve strategies. During the pressure measurements, the engine was run at four bar IMEP,net. The air-fuel ratio is altered by opening or closing the throttle while keeping the fuel injection time nearly constant.

7.1 Pumping mean effective pressure

Figures 37 and 38 show the mean effective pressure as a function of air-fuel ratio. It can be seen that the general trend is lower PMEP for higher air-fuel ratios. This is reasonable since PMEP is a measure of the pumping losses, and the throttle is used less for higher air-fuel ratios.

In the two inlet cam case, the PMEP decreases as the cam phasing is retarded except for the very late inlet cam phase where there is a slight increase in PMEP. In the valve deactivation case, the PMEP is nearly unchanged for the different valve timings, with a slight increase for the very late phase. It can also be noted that the negative gradient of the PMEP is almost twice as large in the two inlet cam case as in the valve deactivation case. This is probably due to the reduced valve opening area with valve deactivation. The same amount of air (as in the two valve case) is forced through one valve, resulting in a pressure drop over the valve — this is called valve throttling.

7.2 Combustion duration

The duration for 0-10% burnt (called ignition delay) and 10-90%burnt (called combustion duration) is seen in Fig. 39-42. In both cases the combustion duration increased with increasing air-fuel ratio, but in the case of valve deactivation the trend is less evident. The ignition delay and combustion duration was shorter for the valve deactivation case and shortest for the very late phase. This is expected since the levels of turbulence was higher in the valve deactivation case and highest in the very late phase. It can be noted that the combustion duration for the two valve case, normal timing and $\lambda = 1$ was longer than the combustion duration for the valve deactivation case with very late cam phase and $\lambda = 1.8$. This was not expected.

7.3 Combustion stability

As could be seen above, the combustion duration was strongly influenced by the turbulence. It is also expected that the combustion stability increases with increasing turbulence. The measure of combustion stability was chosen to be the COV,imep. Figures 43 and 44 show the COV,imep as a function of air-fuel ratio. In the two inlet cam case, the combustion starts to deteriorate at leaner mixtures than $\lambda = 1.5$. In the valve deactivation case the combustion limit can not be seen in the figure. The reason why the latest inlet cam phase and valve deactivation did not have the most stable combustion is probably due to the

large fluctuations in the turbulence from cycle to cycle. This gives large variations in the combustion which leads to decreased combustion stability.

8 Discussion

The results presented in this paper show that the use of an optical access through the side of the pent roof combustion chamber is an attractive way to gain information on the flow situation in a working engine. The major benefit is the possibility to operate the engine at any condition without taking special care to the optical components. This advantage has not been fully realized in the present study but still exists. The use of simultaneous flow and pressure measurements are also a possibility to explore.

The results also show that changes of the gas exchange process will have a major impact on the in-cylinder flow and combustion. Inlet valve deactivation is an effective means of increasing the turbulence level in the cylinder and if the phase of the inlet camshaft is set late this effect will be even more pronounced. The most unexpected behavior was, however, the decreased turbulence level with a late inlet phase without valve deactivation. That made this operation condition much less attractive.

9 Conclusions

Several conclusion can be made from this paper. They are listed below without being ranked in any order.

- Inlet valve deactivation gave higher levels of turbulence which also gave a faster combustion and higher combustion stability.
- PMEP was reduced when the engine was operated lean. This results from less throttling of the engine.
- PMEP was not reduced as much with lean operation and inlet valve deactivation. This is probably due to valve throttling, which appears when large air flows are forced through the single valve.
- Late phasing of the inlet cam and inlet valve deactivation gave very high turbulence. It made the engine operate well even with a very lean mixture ($\lambda = 1.8$).
- Late phasing of the inlet cam with the standard double cam resulted in a decrease in turbulence. That makes this configuration unattractive.

10 Additional work

The continuation of my work is a more thorough study of variable valve timing and lift. We are interested in knowing the difference between various valve strategies and their influence on in-cylinder flow and combustion. Firstly, we are considering comparing the load 4 bar IMEP,net for late inlet valve closing, early inlet valve closing and some asymmetric valve strategies. For this reason I wrote a Matlab macro to easily calculate different cam lobe designs when the duration and lift was known. The Matlab macro is given in the appendix of this work.

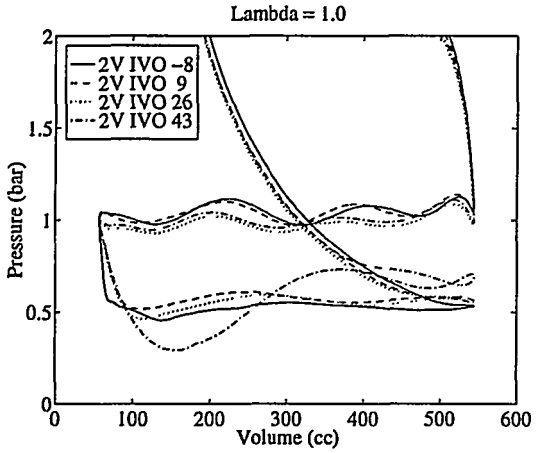

Figure 33: P-V diagram for different inlet cam phases with both inlet valves active.

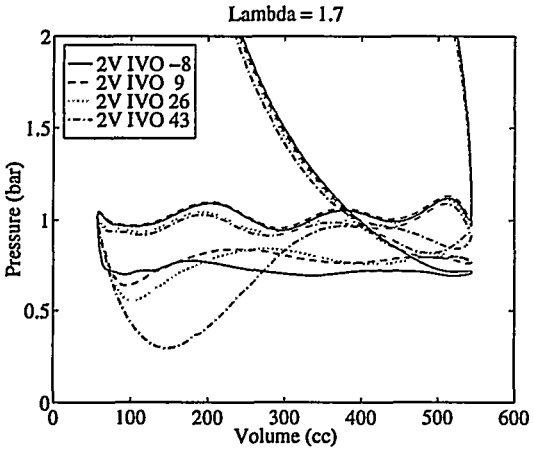

Figure 34: P-V diagram for different inlet cam phases with both inlet valves active.

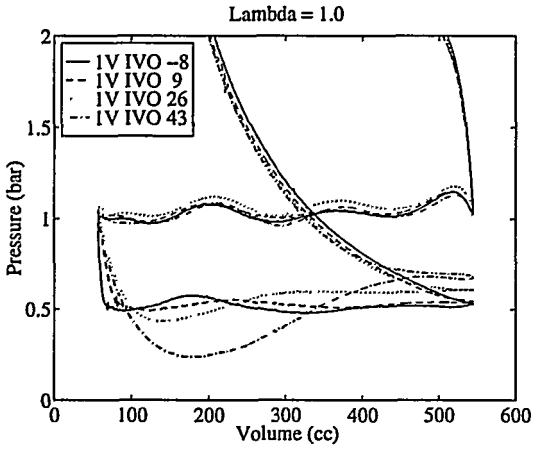

Figure 35: P-V diagram for different inlet cam phases with valve deactivation.

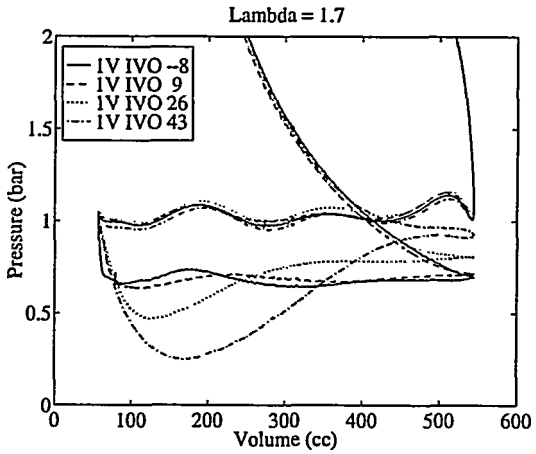

Figure 36: P-V diagram for different inlet cam phases with valve deactivation.

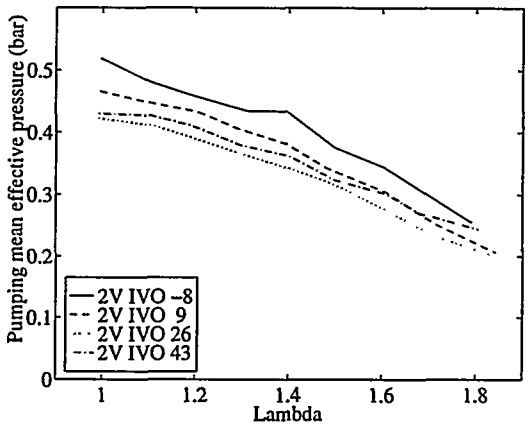

Figure 37: Pumping mean effective pressure for different cam phases with both inlet valves active.

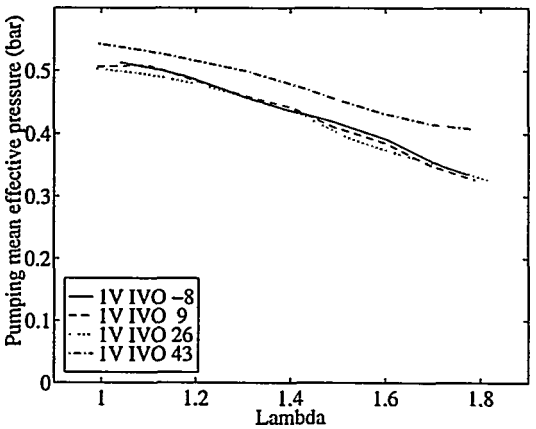

Figure 38: Pumping mean effective pressure for different cam phases with valve deactivation.

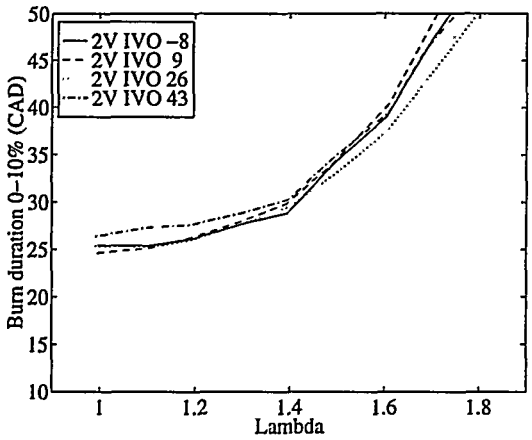

Figure 39: Duration of ignition delay (0-10% heat released) for different cam phases.

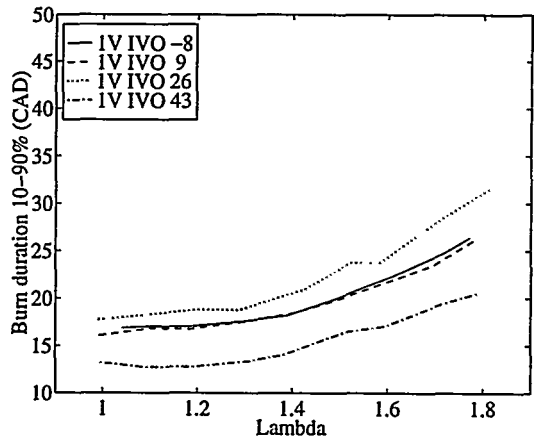

Figure 42: Combustion duration (10-90% heat released) for different cam phases and valve deactivation.

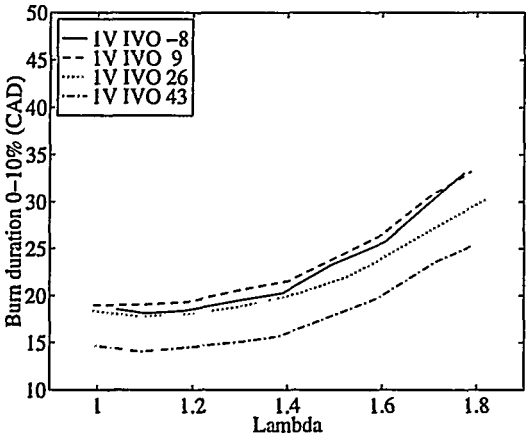

Figure 40: Duration of ignition delay (0-10% heat released) for different cam phases and valve deactivation.

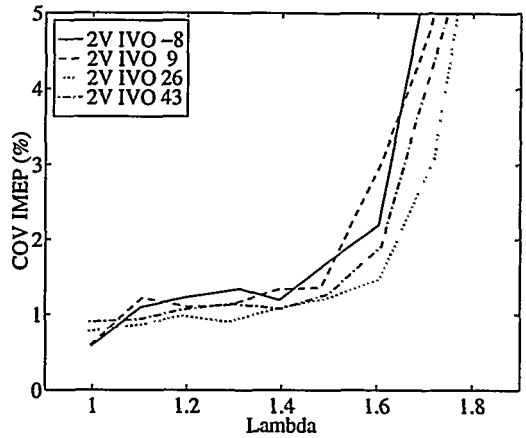

Figure 43: Variation of net indicated mean effective pressure for different cam phases.

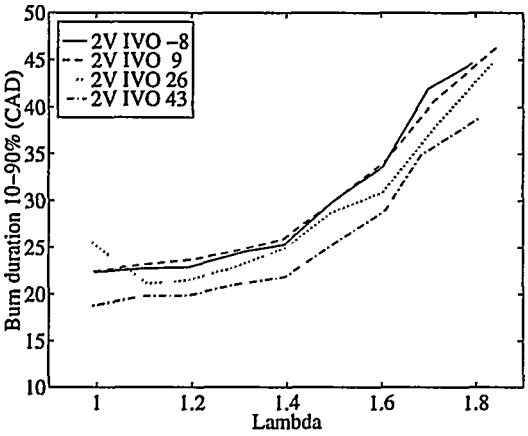

Figure 41: Combustion duration (10-90% heat released) for different cam phases.

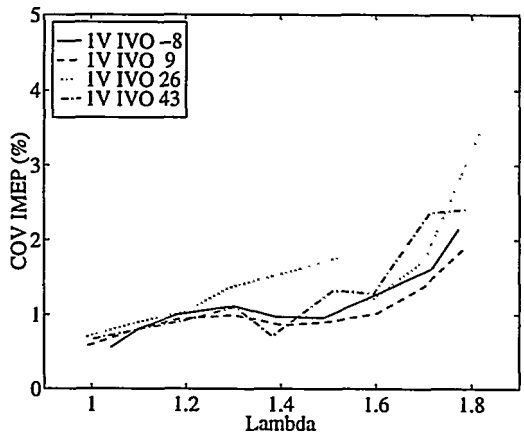

Figure 44: Variation of net indicated mean effective pressure for different cam phases and valve deactivation.

11 References

[1] K. Horie, K. Nishizawa, T. Ogawa, S. Akazaki, K. Miura; "The Development of a High Fuel Economy and High Performance Four-Valve Lean Burn Engine", SAE920455

[2] M. Grohn, K. Wolf from Mercedes-Benz AG; "Variable Valve Timing in the new Mercedes-Benz Four-Valve Engines", SAE891990

[3] M. M. Schechter, M. B. Levin; "Camless Engine", SAE960581

[4] http://www.nissanmotors.com; The homepage of Nissan in USA.

[5] M. Klell, A. Wimmer; "A Procedure for a Thermodynamic Valuation of Pressure Transducers", MTZ Motortechnische Zeitschrift 50, 1989 (In German)

[6] B. Johansson; "On Cycle to Cycle Variations in Spark Ignition Engines - The Effects of Fluid Flow and Gas Composition in the Vicinity of the Spark Plug", 1995

Appendix

Cam profile calculation program

This is a presentation of the cam profile calculation program written by me, Fredrik Söderberg, as a Matlab-file. Below is a graph indicating the structure of the program and the location of the files. The files are executed downwards, and from left to right.

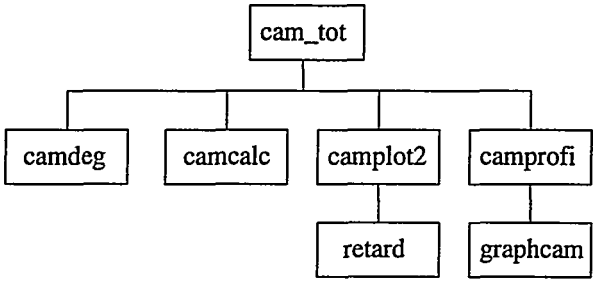

Additional files:

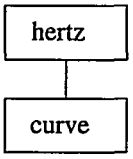

The location of the files is: c:\fredrik\matlab\m-filer\

```
% This m-file runs the entire cam profile calculation and plotting
% program, making plots and graphs. For more information see help
% in respective sub-routines listed below.

camdeg
camcalc
camplot2
camprofi
```

```
% This file contains all necessary data on the cam lobe.
%
% Description of parameters:
%
% Ss0E [mm/rad] = the speed of the valve when the clearance has been lifted
% H [mm] = total lift
% z = describes the curve form for the retardation, chosen to be 5/8
%     according to Bensinger's book
% Fi0 [deg] = duration of clearance lift
% Fi1 [deg] = duration of acceleration period
% Fi2 [deg] = duration of first retardation period
% Fi3 [deg] = duration of second retardation period
% duration [deg] = Fi1+Fi2+Fi3, total duration
% H0 [mm] = clearance lift, chosen to be 0.12 mm (by adjusting Fi0 and Ss0E)
% rb = base circle radius

clear;   % Clears all parameters before running the program.

rb = 16;
Ss0E = 1.35;
z = 5/8;

Fi0 = 8; % Never change Fi0 !!

H = 9.0;
Fi1 = 19;
duration = 154;

Fi2 = round((duration*0.5-Fi1)/11);
Fi3 = 0.5*duration-Fi2-Fi1;


H0 = Ss0E*2*Fi0*(pi/180)/pi;

```

```
% This m-file calculates coefficients necessary for determining
% the shape of the acceleration curve and hence the lift curve.
% (Bensinger, Die Steuerung des Gaswechsels in schnellaufenden
% Verbrennungsmotoren 1968, pp 40-42)

k1 = 8*z*(Fi2*pi/180/pi)^2;
k2 = (5+z)*(Fi3*pi/180)^2/6;
k3 = (4+2*z)*Fi3*pi/180/3;
K1 = k1 + k2 + k3*Fi2*pi/180;
K2 = k3 + 4*z*Fi2*pi/180/pi;

c11 = (K1*Ss0E + K2*H)/(2*K1 + K2*Fi1*pi/180);
c12 = (c11 - Ss0E)*Fi1*pi/180/pi;
c32 = (2*c11 - Ss0E)/K2;
c21 = c32*k3;
c22 = c32*k1;
c31 = c32*(1-z)/(6*(Fi3*pi/180)^2);
c33 = c32*k2;

s1E = H0 + c11*Fi1*pi/180;
s2E = s1E + c21*Fi2*pi/180 + c22;
Htot = s2E + c33;

% Control of calculated results. The second expression shall be equal to
% Ss0E and the other expressions shall be zero.

c31*(Fi3*pi/180)^4 - c32*(Fi3*pi/180)^2 + c33
c11 - c12*pi/(Fi1*pi/180)
c11 + c12*pi/(Fi1*pi/180) - c21 - c22*pi/(2*Fi2*pi/180)
c21 + 4*c31*(Fi3*pi/180)^3 - 2*c32*Fi3*pi/180
c22*(pi/(2*Fi2*pi/180))^2 + 12*c31*(Fi3*pi/180)^2 - 2*c32
```

```
% This m-file plots the lift curve, the velocity curve and the
% acceleration curve. Lift data is inserted in s(fi), velocity data
% is inserted in vel(fi) and ss(fi) and acceleration data is inserted
% in acc(fi) and sss(fi). ss(fi) and sss(fi) are used to calculate
% the curvation of the finished cam profile.

for Fi = 0:(duration/2+Fi0)
   if ((0 <= Fi) & (Fi < Fi0))
      % do nothing
   elseif ((Fi0 <= Fi) & (Fi <= Fi0+Fi1))
      s(Fi+1) = H0 + c11*(Fi-Fi0)*pi/180 - c12 *
         sin((pi/(Fi1*pi/180))*(Fi-Fi0)*pi/180);
      ss(Fi+1) = c11 - c12*pi/(Fi1*pi/180) *
         cos(pi/(Fi1*pi/180)*(Fi-Fi0)*pi/180);
      sss(Fi+1) = c12*(pi/(Fi1*pi/180))^2 *
         sin(pi/(Fi1*pi/180)*(Fi-Fi0)*pi/180);
   elseif (Fi0+Fi1 < Fi & Fi <= Fi0+Fi1+Fi2)
      s(Fi+1) = s1E + c21*(Fi-Fi0-Fi1)*pi/180 + c22 *
         sin((pi/(2*Fi2*pi/180))*(Fi-Fi0-Fi1)*pi/180);
      ss(Fi+1) = c21 + c22*pi/(2*Fi2*pi/180) *
         cos(pi/(2*Fi2*pi/180)*(Fi-Fi0-Fi1)*pi/180);
      sss(Fi+1) = -c22*(pi/(2*Fi2*pi/180))^2 *
         sin(pi/(2*Fi2*pi/180)*(Fi-Fi0-Fi1)*pi/180);
   elseif (Fi0+Fi1+Fi2 < Fi) & (Fi <= (duration/2+Fi0))
      s(Fi+1) = s2E + c31*(Fi3*pi/180-(Fi-Fi0-Fi1-Fi2)*pi/180)^4 -
         c32*(Fi3*pi/180-(Fi-Fi0-Fi1-Fi2)*pi/180)^2 + c33;
      ss(Fi+1) = -4*c31*(Fi3*pi/180-(Fi-Fi0-Fi1-Fi2)*pi/180)^3 +
         2*c32*(Fi3-(Fi-Fi0-Fi1-Fi2))*pi/180;
      sss(Fi+1) = 12*c31*(Fi3*pi/180-(Fi-Fi0-Fi1-Fi2)*pi/180)^2 - 2*c32;
   end
end

s(1) = 0;
s(2) = 0.001538461538;
s(3) = 0.008138461538;
s(4) = 0.01993846154;
s(5) = 0.03693846154;
s(6) = 0.0576;
s(7) = 0.0784;
s(8) = 0.0992;
s(9) = 0.12;

% This section makes a mirror image of the lift curve and inserts
% it into the vector s.

if rem(duration,2) ~= 0
   korr = 0.5;
   korr2 = 0;
else
   korr = 1;
   korr2 = 1;
end

counter = 0;
for Fi=(duration/2+Fi0+korr):(duration+2*Fi0)
   s(Fi+1) = s(Fi-2*counter-korr2);
   counter = counter + 1;
end

index1 = -length(s)/2+0.5:1:length(s)/2-0.5;

figure
plot(index1,s);

vel = diff(s);

index2 = -length(vel)/2+0.5:1:length(vel)/2-0.5;

figure
plot(index2,vel);

acc = diff(vel);
acc2 = acc.*(6000/2*pi/30/(pi/180))^2/1000;
index3 = -length(acc)/2+0.5:1:length(acc)/2-0.5;
```

```

figure
plot(index3,acc);

figure
plot(index3,acc2);

hold on;
retard;
```

```
% This m-file requires that you first run the following files:
% camdeg, camcalc and camplot2.
% This file calculates x,y-coordinates for the cam profile
% from the lift data. The problem is how to connect the clearance
% ramp to the lift curve.
%
% Calculation of coordinates for the main lift profile
% Inserting the clearance lift into the vector s
% Since the lift is symmetrical, s is then mirrored.
% vel [mm/deg] = diff(s), velocity-vector
% acc [mm/deg^2] = diff(vel), acceleration-vector
% x [mm] = x-coordinate for the cam-lobe
% y [mm] = y-coordinate for  -  "  -

for Fi = Fi0:duration/2+Fi0
   x(Fi+1) = (rb + s(Fi+1))*cos((90-(duration/2)+Fi-Fi0)*pi/180) -
      ss(Fi+1)*sin((90-(duration/2)+Fi-Fi0)*pi/180);
   y(Fi+1) = (rb + s(Fi+1))*sin((90-(duration/2)+Fi-Fi0)*pi/180) +
      ss(Fi+1)*cos((90-(duration/2)+Fi-Fi0)*pi/180);
end

%  Calculation of coordinates for the clearance lift profile

for Fi = 0:Fi0-1;
   x(Fi+1) = (rb + (s(Fi+2)+s(Fi+1))/2)*cos((90-(duration/2)+Fi-Fi0+0.5)*pi/180) -
      ((vel(Fi+1))/(pi/180))*sin((90-(duration/2)+Fi-Fi0+0.5)*pi/180);
   y(Fi+1) = (rb + (s(Fi+2)+s(Fi+1))/2)*sin((90-(duration/2)+Fi-Fi0+0.5)*pi/180) +
      ((vel(Fi+1))/(pi/180))*cos((90-(duration/2)+Fi-Fi0+0.5)*pi/180);
end

%  Calculation of coordinates for the base circle

for Fi = -90:(90-(duration/2+Fi0))
   xg(Fi+91) = rb*cos(Fi*pi/180);
   yg(Fi+91) = rb*sin(Fi*pi/180);
end;

for Fi = 1:length(xg)+length(x)
   if Fi <= length(xg)
      xtot(Fi) = xg(Fi);
      ytot(Fi) = yg(Fi);
   else
      xtot(Fi) = x(Fi-length(xg));
      ytot(Fi) = y(Fi-length(xg));
   end
end

figure
fullfig8
plot(xtot,ytot,'.',...
   -xtot,ytot,'.');
axis([-28 28 -28 28]);
axis('square');

hold on;

graphcam;
```

```
% This file calculates the spring force for
% a Volvo valve spring. The force is then transformed
% into allowed retardation for the valve, allowed_acc(fi).

disdata = [8.4 17.9];
forcdata = [270 670];

coeff = polyfit(disdata, forcdata,1 );

for i = 1:length(s),
   forc(i) = coeff(1)*(s(i)+8.4) + coeff(2);
   allowed_acc(i) = -forc(i)/0.14576;
end;

plot(index1,allowed_acc);

```

```
% This m-file makes a graphical presentation of the cam profile, to be
% used to verify the theoretical calculations. The cam follower is
% plotted at every cam shaft degree, thus outlining the cam profile.

for Fi = 0:duration + 2*Fi0;
   xpoint(Fi+1) = (rb+s(Fi+1))*cos((90-(duration/2)-Fi0+Fi)*pi/180);
   ypoint(Fi+1) = (rb+s(Fi+1))*sin((90-(duration/2)-Fi0+Fi)*pi/180);
   p_one(Fi+1,1) = xpoint(Fi+1)-16*sin((90-(duration/2)-Fi0+Fi)*pi/180);
   p_one(Fi+1,2) = xpoint(Fi+1)+16*sin((90-(duration/2)-Fi0+Fi)*pi/180);
   p_two(Fi+1,1) = ypoint(Fi+1)+16*cos((90-(duration/2)-Fi0+Fi)*pi/180);
   p_two(Fi+1,2) = ypoint(Fi+1)-16*cos((90-(duration/2)-Fi0+Fi)*pi/180);
end

plot(p_one(1,:),p_two(1,:));
hold on;
for i = 2:duration+2*Fi0+1
   plot(p_one(i,:),p_two(i,:));
end
```

```
% To run this file, you have to run cam_tot first.
% This file determines the contact pressure according
% to Hertz, by using the curve radius and the force exerted
% by the cam.

curve;
mass = 0.14576;
for n = Fi0:duration/2+Fi0
   Ffj = forc(n);
   Facc1 = mass*sss(n)*((3000*pi/30)^2)/1000;
   Facc2 = mass*sss(n)*((500*pi/30)^2)/1000;
   F1(n) = abs(Ffj + Facc1);
   F2(n) = abs(Ffj + Facc2);
   b1 = 1.52*((F1(n)*curve_radius(n))/(211e3*14))^0.5;
   b2 = 1.52*((F2(n)*curve_radius(n))/(211e3*14))^0.5;
   SigmaH1(n) = 0.637*F1(n)/(b1*14);
   SigmaH2(n) = 0.637*F2(n)/(b2*14);
end;

max(SigmaH1)
if max(SigmaH1) == SigmaH1(n)
   disp('Toppvärdet är dimensionerande')
else
   disp('Flankvärdet är dimensionerande')
end

disp('Tomgångsvärde:');
SigmaH2(n)
```

```
% This file determines the curve radius of the cam. cam_tot must
% have been run first.

for m = Fi0:duration/2+Fi0
   curve_radius(m+1) = rb + s(m) + sss(m);
end;

for m=0:Fi0-1
   curve_radius(m+1) = inf;
end;
```